Journal of Hydrology: Regional Studies 17 (2018) 83–94

Contents lists available at ScienceDirect

Journal of Hydrology: Regional Studies

journal homepage: www.elsevier.com/locate/ejrh

Modeling the impacts of changing climatic extremes on streamflow and sediment yield in a northeastern US watershed

J. Stryker[a,*], B. Wemple[b], A. Bomblies[a]

[a] Department of Civil and Environmental Engineering, University of Vermont, Burlington, VT 05405, United States
[b] Department of Geography, University of Vermont, Burlington, VT 05405, United States

ARTICLE INFO

Keywords:
Extreme flows
Suspended sediment
Peak flows
Changing precipitation
Sediment modeling

ABSTRACT

Study region: We investigate the impacts of local temperature and precipitation trends on discharge and sediment loading by applying the model to a watershed in the northeastern US, where trends in increasing precipitation exceed those of other regions in North America.
Study focus: In this study we simulate the response of watershed sediment loading to changing frequencies and magnitudes of extreme precipitation events using a coupled model that explicitly simulates streambank erosion and failure within a distributed watershed model. To drive the model, we use meteorological inputs from general circulation models (GCMs) as well as from a statistical weather generator (WG).
New hydrological insights for the region: Changes in the timing and magnitude of snow melt and spring flows, as well as associated sediment mobilization, resulted from increases in temperature. Increases in discharge and sediment load resulted from increases in precipitation events exceeding the 95th percentile. In runs driven by WG weather data, positive trends were evident in peak (as well as annual) discharge and suspended sediment yields over the years modeled. No clear trends were seen in GCM-driven runs, which do not capture historically-observed trends in extreme precipitation. This work is consistent with other studies in that it shows important changes in discharge and sediment yields from a watershed resulting from ongoing changes in climate.

1. Introduction

Changing weather patterns will have complex and nonlinear impacts on many human and environmental systems, including on processes governing the mobilization and transport of sediment within watersheds. Significant increases in the frequency of extreme precipitation events have been documented in the United States (Karl and Knight, 1998; Kunkel et al., 1999; Kunkel, 2003; Guilbert et al., 2015). Although relationships between sediment loading and discharge vary among watersheds (Webb and Walling, 1982; Williams, 1989; Asselman, 1999; Hamshaw, 2014), extreme precipitation and/or resulting flow events result in disproportionately higher suspended sediment loading in transport limited systems (Gonzalez-Hidalgo et al., 2010; Oeurng et al., 2010). Increased sediment yields resulting from such events can exceed the capacity of existing infrastructure, as well as result in the increased transport of sediment-bound nutrients to receiving water bodies. One of the mechanisms by which sediment is mobilized, particularly in response to high precipitation and flow events, is through streambank erosion and failure. These processes, though widely observed, have not heretofore been widely included in watershed models. Efforts to integrate streambank erosion and phosphorus mobilization are important in watershed model development for assessments (Mittelstet et al., 2016), particularly in the context of

* Corresponding author.
E-mail address: jstryker@stone-env.com (J. Stryker).

https://doi.org/10.1016/j.ejrh.2018.04.003
Received 4 April 2017; Received in revised form 13 February 2018; Accepted 13 April 2018

understanding the impacts of climate change and increasing extremes.

Increased sediment loading due specifically to streambank erosion can not only contribute large amounts of sediment-bound phosphorus and other nutrients (Kronvang et al., 2012, 1997), but can also negatively impact water quality both in the watershed and further downstream. The contributions of bank erosion have been investigated in the northeastern United States by authors including Langendoen et al. (2012), DeWolfe et al. (2004), Morrissey et al. (2011), Nagle et al. (2007), and others. Accelerated streambank erosion can contribute to disproportionate sediment supply to specific areas of a watershed, stream channel instability, land and habitat loss, water quality degradation, as well as other consequences (US EPA, 2012). In addition, erosion and undercutting of banks and the continued incision of streams can affect the flood resiliency of adjacent areas and infrastructure. Both heavy rainfall and high flows from snowmelt driven by temperature variability can result in adverse impacts. Therefore, ability to model the combination of conditions (watershed state and precipitation) that give rise to high loadings under changing extremes would advance understanding of stream, watershed, and receiving water body response to changing precipitation extremes.

Computational techniques have been used to understand the physical processes and mechanisms responsible for observable changes in the environment. One of the advantages of developing physics-based modeling approaches is the capability of simulating scenarios that are outside the range of those previously observed. Stryker et al. (2017) coupled the Distributed Hydrology Soil Vegetation Model (DHSVM) (Wigmosta et al., 1994) and the Bank Stability and Toe Erosion Model (BSTEM) (Simon et al., 2000, 2003, 2011) in order to better represent the mechanistic processes governing streambank erosion and failure within a distributed watershed model. DHSVM is a distributed watershed model that simulates water and energy fluxes at sub-daily time steps. DHSVM has been used extensively to evaluate impacts of environmental change as well as anthropogenic land use change, such as from urbanization and deforestation, on watershed hydrology (Leung and Wigmosta, 1999; Bowling et al., 2000; Whitaker et al., 2002; Cuo et al., 2009; Lanini et al., 2009; Safeeq and Fares, 2012). This model also incorporates the mobilization of sediment due to overland and road erosion in response to precipitation, and the transport of sediment across the land surface and within the stream network (Doten et al., 2006). BSTEM was chosen for its advanced, physics-based representation of both hydraulic and geotechnical processes that play a role in erosion and bank failure. It consists of two components: a toe erosion module to simulate undercutting of banks by streamflow and a bank stability module to assess the likelihood of failure and the most likely failure plane. The representation of bank undercutting, resulting from fluvial erosion as a function of excess shear stress, is critical to accurate simulation of bank stability (Simon et al., 2000), particularly for examining changing flow regimes. In addition, BSTEM simulates the physical characteristics of soils, including negative pore pressures that can develop in unsaturated soil conditions. Since warmer temperatures are likely to affect soil moisture balances, the ability to simulate the role of these processes on bank stability is also significant. This improved modeling approach is therefore suitable for investigating the impact of climate change scenarios and the occurrence of extreme events on the hydrology and sediment mobilization in small- (10^0–10^1 km^2) and meso- (10^1–10^2 km^2) scale watersheds.

In order to simulate the impacts of climate change, however, such models require specific meteorological inputs that reflect the anticipated deviations in climate variables, particularly temperature and precipitation. Several studies have shown that precipitation in the United States, and in the Northeast region specifically, is increasing and becoming more variable in magnitude (Kunkel et al., 1999, 2013; Kunkel, 2003; Groisman et al., 2005; Guilbert et al., 2015). Kunkel et al. (2013) also projected that temperatures in this region will continue to increase between approximately 2 and 6 °C by 2080 at current emission rates, and that heavy precipitation as well as drought risk will continue to increase. Authors have also found evidence of a signficiant increase in precipitation occurring as extreme precipitation events (heaviest 1% of rainfall) over the last approximately 50 years (e.g. Karl et al., 2009; Groisman et al., 2001, 2012). Regional or local trends are critical for investigating impacts of climate change on human life and ecosystem response (Katz and Brown, 1992; Hayhoe et al., 2006, 2008). Furthermore, global circulation model (GCM) data, including the Coupled Model Intercomparison Project phase 5 (CMIP5) data do not capture historically observed trends and variability in precipitation in some regions of the northeast (Guilbert et al., 2014; Mohammed et al., 2015).

Another challenge to simulating the impacts of climate change at the watershed scale is the temporal resolution of most climate projection data. For example, Xu (1999), Xu et al. (2005), and Prudhomme et al. (2002) noted that GCM products are not adequate for driving hydrological models, in part because they perform poorly at subdaily and even daily time steps. Particularly in mountainous watersheds, storm events often pass within a day, leading to high temporal variability in water and sediment fluxes not captured in models operating on daily time steps. A number of approaches exist to address the unsuitable spatial and temporal scale of GCMs, including regional climate models, hypothetical scenarios, and both dynamic and statistical downscaling techniques (Xu, 1999). Alternative methods to GCMs, such as statistical weather generators (WGs), may be better suited for the prediction of future temperature and precipitation data for specific regions. Although these techniques have been applied to watershed modeling, these approaches also have limitations and key challenges still exist in using existing climate data products to simulate impacts of future trends in settings like this.

Our application is set in a region where changes in extreme precipitation are well documented. The watershed encompasses high-gradient headwater forested streams and agricultural floodplains. Post-glacial alluvial sediments dominate the landscape and its history includes significant anthropogenic changes in land use (such as deforestation) and to stream channels (such as mill dams and channelization), making it susceptible to impacts of high precipitation and flow events (Whalen, 1998; Barg and Blazewicz, 2003; Dunn et al., 2007a,b; Nagle et al., 2007; Walter and Merritts, 2008). Again, subdaily simulation is critical for capturing the dynamic processes in such watersheds and understanding the influences of changes in precipitation and temperature.

In the context of this paper, extreme precipitation events are characterized as those resulting in daily flows that exceed the 95th percentile. This work goes beyond using downscaled GCM output to also using temperature and precipitation data created with a statistical WG that captures local trends and variability in precipitation to drive model runs. We apply a physically-based watershed model to investigate impacts of increases in temperature and extreme precipitation magnitude and frequency on flow and sediment

production dynamics in a meso-scale, high-gradient watershed. The primary goal of this study is to assess the hydrological and sediment related impacts of climate change in a representative northeastern US watershed, particularly with respect to the increased occurrence of extreme events. The secondary purpose of this study is to assess the ability of these climate products to reflect the non-stationary shifts in climate that are occurring in this region, and the resulting alterations in hydrologic and sediment-related processes at a watershed-scale.

2. Methods

This study examines hydrological- and sediment-related simulations produced by the coupled DHSVM-BSTEM model (Stryker et al., 2017) and driven by two sets of meteorological inputs. The hydrology model (DHSVM) mechanistically simulates watershed hydrology (Wigmosta et al., 1994) and uses a 4-point finite difference scheme based on Wicks and Bathurst (1996) to move sediment downslope through a channel network, where sediment is binned by size and routed independently (Doten et al., 2006). Transported load includes changes in stored sediment as well as suspended sediment, and total transport is limited by Bagnold's equation (Bagnold, 1966). Based on BSTEM v5.4, toe erosion and undercutting of channels is calculated as a function of excess shear stress and a force equilibrium analysis used to estimate a Factor of Safety (*FoS*) (Simon et al., 2011). If the bank fails, sediment that enters the stream channel is routed downstream with other local stream flows (eroded sediment from roads, overland sediment, sediment from upstream, and suspended sediment).

The study site was the Mad River watershed in Central Vermont, which drains approximately 373 km^2 of land and is bordered by the Green Mountains. Land use in the watershed was assumed static for the purposes of focusing on the impacts of specific changes in climate, where 86.5% was classified as mixed forest, 2.1% as roads, 5.5% as urban/residential, and 4.4% as agricultural (including crops, pasture, and hay) based on the 2006 National Land Use Cover Dataset (NLCD). Stryker et al. (2017) demonstrated the ability of the coupled model to represent sediment mobilization from watershed sources, particularly in response to larger precipitation and flow events. To evaluate model performance in that work, simulated sediment loads for the entire watershed were compared to load estimates based on measured suspended solids at the outlet of the watershed. Model simulated concentrations at the outlet of several subbasins were compared to measured concentrations at those locations. The same model calibration presented in that work was used here; all spatial input files and parameter values are as described by Stryker et al. (2017).

The Mad River watershed drains to Lake Champlain, a freshwater lake situated between Vermont, New York, and Canada. Lake Champlain has experienced an increase in frequency of summer harmful cyanobacteria algae blooms (Watzin et al., 2010), which is in agreement with expected impacts of climate change for many freshwater lakes (Whitehead et al., 2009; Moss, 2012; El-Khoury et al., 2015). Regional climate change trends in the northeastern United States and the Lake Champlain Basin, including warming temperatures (particularly in winter) and increased persistence and variability in precipitation events, are more pronounced than global trends (Frumhoff et al., 2007; Stager and Thill, 2010; Guilbert et al., 2015). In Vermont specifically, Betts (2011) has documented several indicators of warming temperatures, including a shorter freeze periods and longer growing seasons over the last 50 years. In addition to experiencing climate trends representative of the northeastern United States, this watershed is also representative of northern New England watersheds that have steep headwaters draining to floodplains with a history of deforestation for agriculture. Peak flows in this region typically occur in the spring, where snow melt has a significant impact on flow magnitude in addition to spring precipitation. Tropical Storm Irene, which affected Vermont in August 2011 following a heavy spring rainfall, is an example of an extreme event that caused significant impacts to the Lake Champlain Basin. This event caused tributary flooding, intense lateral erosion of streambanks, long term changes to river channels and valley morphology, and significant damage to bridges, stormwater infrastructure, and private property (Pealer, 2012; Lake Champlain Basin Program, 2013). This event also resulted in large pulses of potentially nutrient-laden sediments to Lake Champlain.

2.1. Climate data

Using the calibrated DHSVM-BSTEM model for the Mad River watershed, model runs were conducted for the water years (01 Oct–30 Sept) 2020, 2030, 2040, 2050, 2060, 2070, 2080, 2090, and 2099. Each of these water years was preceded by a 10-month spin-up period (01 Jan–30 Sep) to set initial state variables. Two sets of climate temperature and precipitation data were used to drive the model.

The first set of this data was developed by Winter et al. (2016) and based on the output of GCM simulations. Winter et al. used simulations from phase 5 of the Coupled Model Intercomparison Project (CMIP5) multimodel ensemble downscaled to an intermediate resolution using the bias corrected with constructed analogs (BCCA) method (Brekke et al., 2013) as the basis for further downscaling. The BCCA ensemble included 20 GCMs run as part of CMIP5 under two representative concentration pathways (RCPs) (Moss et al., 2010). Winter et al. (2016) further downscaled that data set specifically for a mountainous region in the Northeast that included our study area, by using empirical relationships between elevation and daily maximum and minimum surface temperature and precipitation from local station data. The result was gridded maximum and minimum surface temperatures, as well as precipitation, available at a daily time step for 1950–2099. For this work, we chose four locally downscaled GCM scenarios for RCP 8.5, representing the 90th percentile of the reference emissions range and similarly representative of greenhouse gas and particle emissions resulting in greater than 8.5 W/m^2 of radiative forcing in 2100 (Moss et al., 2010). We used a warm scenario, a cool scenario (2nd coolest of RCP8.5), a wet scenario, and a dry scenario. These scenarios are meant to bracket future climate trajectories.

The second set of data were developed by White et al. (in press) using a statistical WG. White et al. generated meteorological time maximum and minimum daily temperature and daily precipitation using a Markov-chain Monte Carlo approach with non-stationary

precipitation and extreme precipitation distributions. This method incorporated the trends noted by Guilbert et al. (2015) to generate a precipitation time series that statistically reflects the changing probability of extreme events and allows for increasing variance and skewness in the precipitation distribution looking into the future. These data were available for the years 2011–2050. For this work we randomly chose 100 realizations from the time series produced by White et al. (in press) for the water years 2020, 2030, 2040, and 2050 to drive the watershed model.

Although simulated runoff and streamflow are most affected by temperature and precipitation, DHSVM requires additional meteorological inputs including humidity, wind speed, incoming longwave radiation, and incoming shortwave radiation. These variables affect energy and carbon fluxes, vegetation processes, and other model processes. To complete the meteorological inputs (wind speed, humidity, incoming longwave radiation, and incoming shortwave radiation) required for the coupled hydrology bank stability model we used National Centers for Environmental Protection (NCEP) Reanalysis data provided by the NOAA/OAR/ESRL PSD, Boulder, Colorado, USA, (http://www.esrl.noaa.gov/psd/). The North American Regional Reanalysis (NARR) data are high resolution combined model and assimilated time series datasets, available at a resolution of eight times daily. NARR data were assessed for a 15-year period spanning 2000–2014 to evaluate interannual variability (see Supplemental information). Data for the period 01 January 2012 through 30 September 2013, representative of this 15-year window, were used in all model runs to complete the meteorology time series.

Climate inputs included both downscaled deterministic GCM-based scenarios (4 scenarios for 9 different years) as well as WG-derived scenarios, which were assessed as an ensemble (100 realizations of temperature and precipitation for each of 4 different years). Due to the long run times, continuous long-term periods were not simulated and results of single water years in 10-year increments were evaluated. We assessed baseline results as the average of 85 realizations of statistically-generated precipitation and temperature for the water year 2012 in order to isolate the impacts of future temperature and precipitation predictions on watershed discharge and sediment. The statistics describing precipitation for the 2012 WG realizations were very similar to those for observed 2011 data and therefore considered representative of a baseline scenario. The meteorological input files for these baseline realizations were then completed with the same NARR 2012 water year variables as future scenario runs.

2.2. Sub-daily model inputs

The coupled watershed model operates most reliability at higher temporal resolutions, particularly for the purpose of simulating dynamic hydrology and sediment in mountain settings such as our study site. Therefore, it was necessary to generate subdaily inputs based on the daily data from Winter et al. (2016) and White et al. (in press). Chow and Levermore (2007) described several methods for creating hourly temperature from daily maximum and minimum temperatures ($T_{\max}$ and $T_{\min}$, respectively), as well as an improved method using average daily temperature. In this work we used the sin (14R-1) method for linked days as described by Chow and Levermore, where $T_{\max}$ was set to occur at 2 p.m. and $T_{\min}$ to occur one hour before sunrise. Hourly temperature was calculated as

$$T(t) = \left(\frac{Temp_{next} + Temp_{prev}}{2}\right) - \left[\left(\frac{Temp_{next} - Temp_{prev}}{2}\right) \times \cos\left(\frac{\pi(t - t_{prev})}{(t_{next} - t_{prev})}\right)\right],$$

where $Temp_{next}$ is the next known temperature value (either $T_{\max}$ or $T_{\min}$); and $Temp_{prev}$ is the next known temperature value (either $T_{\max}$ or $T_{\min}$); t_{next} is the time for the next known temperature value, and t_{prev} is the time for the previous known temperature value, and t is the time. Sunrise and sunset times were calculated according to the latitude of the study site based on a standard formula described in Scharmer and Greif (2000).

Sub-daily precipitation inputs were generated from daily GCM and WG data by matching predicted storms to existing storms and partitioning the rainfall similarly through the duration of the storm. Quality-controlled historical hourly precipitation data from the Burlington International Airport weather station in Burlington, Vermont were downloaded from NOAA's National Climatic Data Center (NCDC: http://www.ncdc.noaa.gov). These data span the period 01 May 1948 through 30 November 2011. We analyzed statistics of historical precipitation events from this dataset, including the total duration and depth of each storm (in days), as well as the percentage of the total depth that fell in each day and hour of the event. For each future precipitation scenario (at daily resolution), we found the location (in the time series) and magnitude of all non-zero values, to identify individual precipitation events. For each precipitation event, we calculated daily statistics including duration, depth, and percentage of rainfall that fell in each day of an event. For a one-day event, we sampled a one-day historical precipitation event of the same depth from the Burlington data. If no equal depth was found, we averaged five storms with the closest total depths. For a two-day event, we sampled an existing storm that matched the total depth and the percentage of rain that fell in each day. If we found no exact depth match, we averaged the 10 storms with the closest depths. If we found no equal percentages, we averaged the five storms with the most similar distribution of rainfall. If the storm persisted for longer than two days, we searched the historical record for a matching event. If we identified no suitable precipitation event, then we used a combination of shorter duration precipitation events to generate a suitable event. To accomplish this, we sampled the longest existing storm that matched the depth of equal duration during the daily predicted storm first, then sampled other existing storms of similar depth to fill in the time remaining in the predicted storm. Once we matched each precipitation event with a historical event or combination of historical events, we added or subtracted tenths of millimeters of precipitation from random locations within the event to match the total storm depth from the future precipitation events.

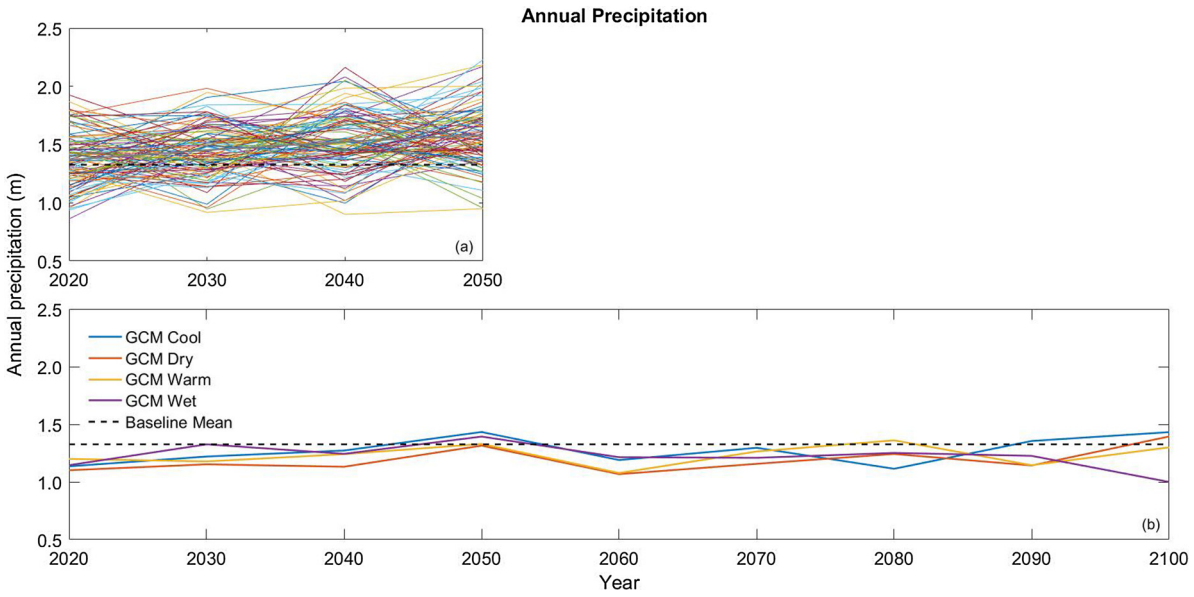

Fig. 1. Annual precipitation in climate change scenarios, where panel (a) shows WG realization totals in comparison to the baseline mean and panel (b) showed GCM scenarios in comparison to the same baseline mean. Baseline mean was calculated as the mean of 85 WG realizations of 2012.

3. Results

Temperature and precipitation scenarios had clear influences on simulated hydrologic processes, including snow accumulation and melt, discharge, and sediment mobilization. Modeled climate trends show differences deriving from the GCM and WG data; we present these, followed by resulting differences in flow and sediment. We investigate results representative of changes in extreme flow and sediment yield, where 'extreme' indicates those results exceeding the 95th percentile.

3.1. Climate trends

Clear differences are evident in the climate time series produced by the alternate methods employed here. WG-derived precipitation shows an increase in annual precipitation as well as a slight trend in the 95th percentile of daily precipitation over the period of 2020 through 2050. These trends are not present in any of the GCM scenarios used here. Annual precipitation and extreme precipitation totals in WG realizations are also higher overall than predicted by GCMs for all years simulated. An increasing trend in maximum storm depth is reflected in WG realizations, although these realizations do not reflect longer storm durations. GCM scenarios have a higher number of wet days, although it has been acknowledged that in part due to the coarse spatial resolution, GCMs tend to over predict the number of days experiencing rainfall, with rainfall intensity being lower than stations within the GCM grid cell (Wehner et al., 2010). In particular, GCM data do not reflect the likelihood of increasing extreme events and variability in precipitation patterns evident in observed data for this region (Maurer et al., 2002; Mohammed et al., 2015). In contrast, GCM scenarios do represent historical and expected trends in temperature, whereas WG realizations in this case were designed to not include these trends. Maximum, minimum, and mean temperatures clearly increase over the 2020 through 2099 period in GCM data. A comparison of annual precipitation is shown in Fig. 1, while 95th percentile (extreme) precipitation, annual number of wet days, maximum storm depth, maximum storm duration, as well as maximum and minimum temperatures between WG realizations and GCM scenarios are shown in Figs. S2–S7 in Supplemental information.

3.2. Stream flow

GCM-driven runs show a trend of earlier spring melt and lower cumulative snow water equivalent totals (Fig. 2). The spring day in which total simulated snow water equivalent was < 0.1 cm occurred 17 days earlier in the 2099 'warm' GCM simulation than in the corresponding 2020 'warm' GCM simulation. In WG-driven runs, this date was within 5 days of the baseline average of May 3rd, and we saw no trend between 2020 and 2050 WG-driven simulations, which assume stationary temperature and nonstationary precipitation. The cumulative amount of snow water equivalent over the winter season (total for the watershed) decreased from 2020 to 2099 in all 4 GCM-driven scenarios, from an average cumulative total of approximately 0.31 m in 2020 to approximately 0.20 m in 2099. Snow water equivalent increased in WG-driven runs, from an average cumulative total of approximately 0.24 m in 2020 to 0.27 m in 2050, where baseline 2012 runs had an average cumulative total of approximately 0.24 m.

Trends, or lack thereof, were also apparent in simulated discharge. The WG-driven runs produced a trend in cumulative discharge that reflected the increase in annual precipitation for the modeled watershed (Fig. 3). Cumulative discharge in WG-driven runs

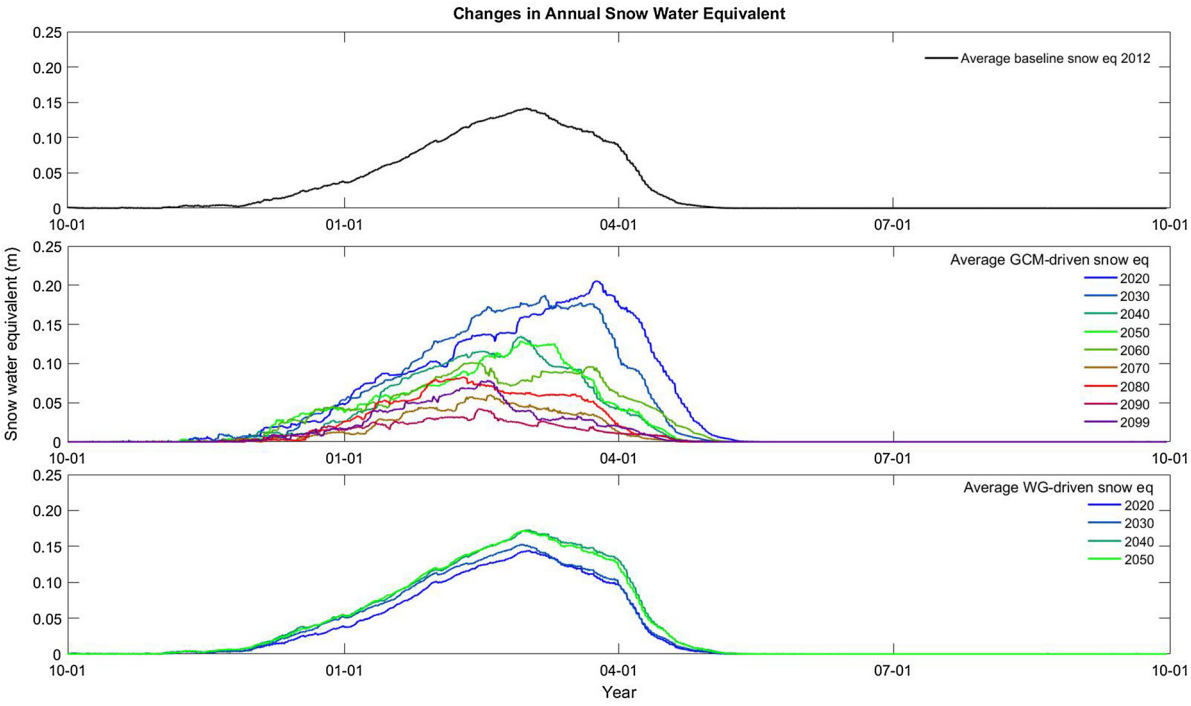

Fig. 2. Snow water equivalent in climate change runs, where average of the GCM scenarios and average of WG realizations are shown in comparison to baseline results.

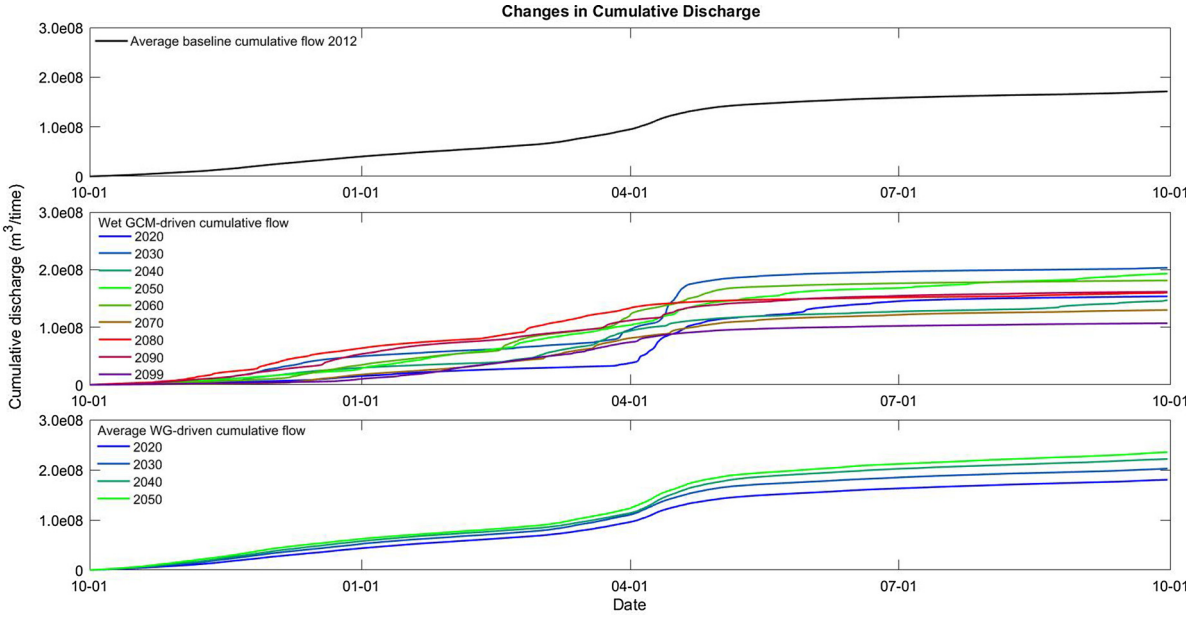

Fig. 3. Cumulative discharge in climate change runs, where results of 'wet' GCM scenario and average of WG realizations are shown.

increased between 2020 and 2050 runs, while GCM-driven runs reflect no clear pattern over time, as expected because of the lack of trends in GCM precipitation. However, warming temperatures have a clear impact on spring melt processes reflected in discharge occurring particularly during the spring where snow melt contributes to high flows. For instance, the 'wet' GCM 2099 simulation resulted in higher discharge throughout the winter period and a less significant increase in cumulative discharge during the typical melt period around April. Spring flows were highest in 2030, and were also high in 2020 GCM scenarios; this was due to rapid warming and resulting snow melt, and consistent with ongoing, observed changes in Vermont and other regions of New England (Betts, 2011; Hodgkins et al., 2002)

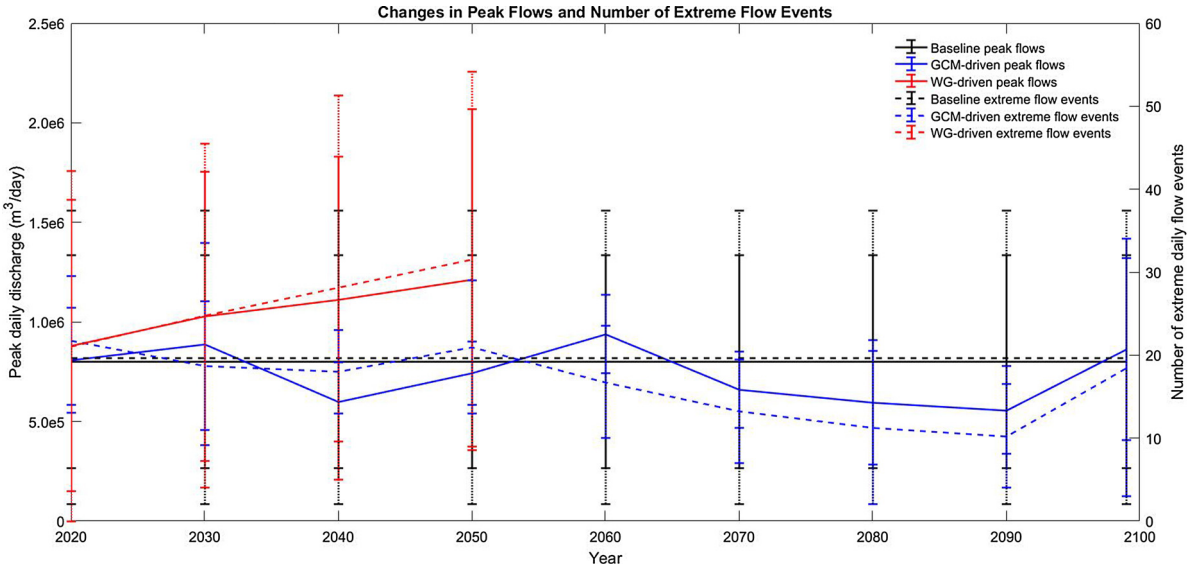

Fig. 4. Peak discharge and number of flow events in climate change simulations, including error bars indicating maximum and minimum peak flows and number of events for each year.

As expected, WG realizations produced higher peak flows and more extreme flows than all GCM scenarios. Average peak flows were higher in WG-driven runs and show an increasing trend between 2020 and 2050 (Fig. 4). We saw no clear trend over time in GCM simulations, reflecting the lack of trend in GCM precipitation. In Fig. 4 we show average peak flows from across the GCM scenarios, WG realizations, as well as the average of baseline scenarios. Peak flows from GCM scenarios were generally similar or less than peak flows seen in baseline simulations. In GCM-driven simulations, peak flow was highest in 2060; peaks seen in the GCM simulations were the result of rapid snow melt in the spring and not a result of extreme precipitation events. In addition, we also show the maximum and minimum peak flows in each year for the different sets of runs (error bars in Fig. 4). WG-driven realizations resulted in more variability in peak flow events than GCM-driven scenarios. The maximum peak flows are also highest in WG-driven runs, although no trend was evident in these maximum values.

WG-driven runs showed a clear increase over time in flows exceeding the 95th percentile of baseline daily discharge (Fig. 4), where GCM-driven runs again showed no obvious trend, and actually decreased between 2050 and 2090. The error bars shown in Fig. 4 also indicate the maximum and minimum number of these extreme events for each year simulated in the different sets of runs. Similarly to the case with peak flows, these indicate that WG-driven runs produce higher maximum flows caused by extreme events in some realizations. GCM scenarios lack representation of high flows caused by extreme precipitation events. The error bars also indicate higher variability in extreme flows.

3.3. Sediment transport trends

Sediment loading in the simulations reflected overall trends in the driving meteorological data as well as modeled discharge. WG-driven runs produced average cumulative sediment loads that were higher than the average baseline cumulative load for all years, and GCM-driven runs produced average cumulative loads lower than the baseline average for most years. No clear trend was seen in GCM-driven runs between 2020 and 2099. As with flow results, cumulative sediment yield was highest in 2030, followed by 2020. Simulated year 2099 did produce the 3rd highest cumulative load of the years modeled. A large increase in cumulative sediment typically occurs in the spring, as a result of spring melt and the associated high flows. This increase was less pronounced or occurred earlier in later years of GCM-driven runs, for example 2099 in the ‘wet’ GCM scenario (Fig. 5). As with discharge, WG-driven runs showed increasing cumulative loads from 2020 through 2050. The model also produced steeper increases in cumulative loads during the summer and fall periods in 2020 and 2030 of the GCM-driven simulations, indicating more sediment mobilization following very high flows in the spring.

Peak sediment loads were also higher in WG-driven runs than in GCM-driven scenarios and baseline realizations. Fig. 6 shows average daily peak sediment flux across the 4 GCM runs, as well as the peak sediment flux from across all WG and baseline realizations. Similar to peak flow, the maximum and minimum peak loads are indicated by the error bars for each set of runs and each year (Fig. 6). The average peak flux in the WG realizations shows an upward trend across the years simulated. Maximum peak fluxes from WG realizations are also significantly higher than those maxima produced by GCM-driven runs, as is overall variability in peak yields (Fig. 6). Alternatively, peak sediment yields generated by the GCM scenarios are generally lower than baseline average peak sediment loads. These also show no increasing or decreasing trend over time.

The number of extreme sediment yielding events follows a similar trend as extreme flow events. As expected, an increasing trend in number of extreme events is evident in WG-driven runs but not in GCM-driven runs. Sediment yields generated by WG realizations

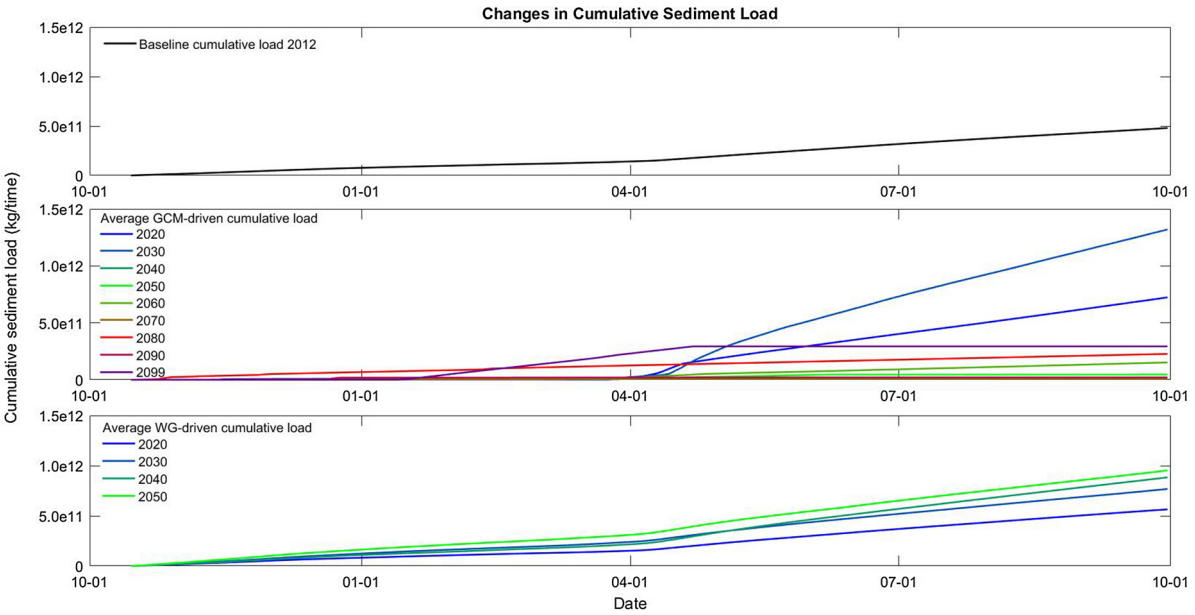

Fig. 5. Cumulative sediment loading in climate change simulations, where the results of the 'wet' GCM scenario and the average of WG realizations are shown in comparison to baseline results.

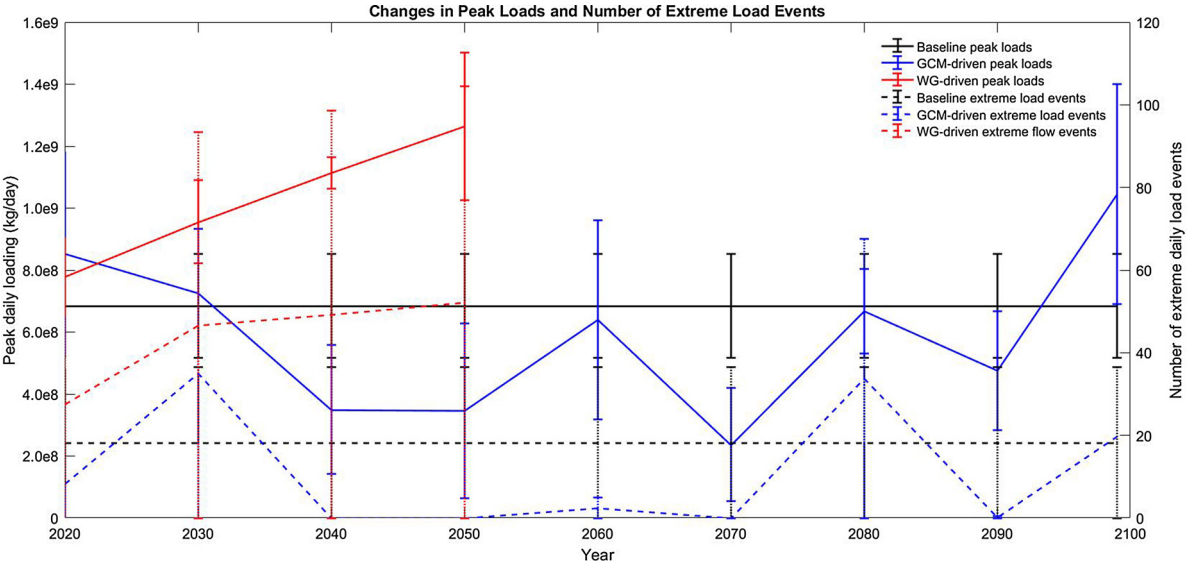

Fig. 6. Peak sediment loads and number of extreme daily sediment loads in climate change simulations, including error bars indicating maximum and minimum peak daily loads and number of extreme daily loads for each year.

also reflect significant variability in comparison to yields generated by GCM scenarios. WG-driven runs also again show the ability to produce conditions leading to years with high numbers of extreme daily sediment loads. WG-driven runs again also show higher variability in the number of days resulting in extreme sediment loads. Generally GCM-driven runs again produced relatively low numbers of extreme daily sediment yields in comparison to baseline and WG-driven runs. There was also significantly lower variability in the GCM-driven sediment yields. The highest number of days with extreme sediment yield occurred in 2030 in GCM-driven scenarios, as a result of very high spring flow.

Almost no change (< 1%) in the mean of the average annual ratio of streambank sediment, relative to other sources of sediment, was seen in either the GCM or WG-driven runs at the watershed outlet. Means of the average annual ratios were calculated as the annual average of ratios calculated at a 3-h resolution for each simulation, and then averaged across all simulations driven by the same weather scenario (Table 1). In baseline, GCM, and WG simulations, the mean average annual ratio of streambank, road, and overland sediment to total sediment at the outlet of the watershed were similar. However, considerable variability was seen in these

Table 1
Ratios of sediment sources at watershed outlet in climate change simulations.

Climate Scenario and Year	Sediment Source	Minimum Average Annual Ratio (%)	Maximum Average Annual Ratio (%)	Mean Average Annual Ratio (%)
Baseline, 2012	Streambanks	74.7	95.0	88.8
	Roads	2.3	18.3	6.8
	Overland	1.8	9.9	4.4
GCM, 2020	Streambanks	84.5	90.3	87.5
	Roads	4.0	10.3	6.6
	Overland	5.1	7.3	5.9
GCM, 2099	Streambanks	81.7	93.0	87.4
	Roads	3.6	11.9	7.2
	Overland	3.3	6.7	5.4
WG, 2020	Streambanks	77.2	95.0	89.1
	Roads	2.3	16.4	6.5
	Overland	2.3	7.7	4.5
WG, 2050	Streambanks	81.3	94.5	89.9
	Roads	2.6	12.5	5.3
	Overland	2.4	8.8	4.8

ratios (both among simulations as well as throughout the year in a single simulation). For example streambank sediment contributions ranged from 74.7 to 95.0%, road sediment ranged from 2.3 to 18.3%, and sediment mobilized by overland flow ranged from < 1.8 to 9.9% of total sediment seen at the outlet under baseline conditions. In this work, model simulated bank collapse did not show the expected non-linear response to changes in climate, and actually showed a linear response close to zero.

4. Discussion

Although the potential impacts of climate change on discharge and sediment mobilization in a watershed are highly variable, it is evident that local trends in precipitation and temperature will have important effects. This study shows the simulated watershed response to increasing precipitation as well as to increasing temperatures. Increasing precipitation in the WG-driven runs caused increases in discharge and sediment loading. This occurred as higher snow totals during the winter, higher flows in the spring, and an increase in more extreme precipitation and resulting flow events that caused higher erosion throughout the simulation period. No overall increase in discharge occurred in the GCM-driven runs, most likely because GCM scenarios did not reflect an observed regional trend in increasing frequency and magnitude of precipitation extremes. However, because of increasing temperatures in the GCM-driven runs, changes in the timing and magnitude of spring melt did occur. The model predicted lower cumulative sediment loading in future years when driven by GCM scenarios, due both to lower flows in spring and fewer extreme precipitation and flow events throughout the summer months.

Stochastic WGs often generate precipitation realizations based on statistical sampling, where other variables may be determined based on their co-occurrence probabilities and the occurrence of wet and dry days (Fowler et al., 2007). We expect that using driving data with representation of both increasing temperatures and precipitation would show more variability over time in the relative contribution of sediment sources. Increasing temperatures and longer storm durations contributing to wetter antecedent conditions might produce more erosion of land surfaces, where extreme precipitation events are likely to particularly increase sediment mobilization from erosion of roads and streambanks. We simulated these changes using the coupled DHSVM-BSTEM model, and although we saw the expected increases in overall sediment yields in response to higher precipitation and increased frequency of events, we saw little change in the ratio of sediment from one source to another. Continued efforts in developing WGs should focus on an approach that can be tailored to specific regions and represent observed trends as well as variability in multiple climate variables. Additionally, approaches targeted at regional dynamic models should be specifically adapted for simulation of smaller scale weather processes.

This study highlights the need for higher resolution meteorological data that reflects local trends in climate, a regionally-variable deficiency in GCMs for the purpose of impacts evaluation. The results presented here clearly show that both temperature and precipitation have a significant influence on discharge and sediment mobilization in a watershed through the behavior of snowpack and soil moisture. Earlier spring snow melt could also result in earlier erosion and incision of banks, making areas more susceptible to spring precipitation events. Representing the trend of increasing storm duration, and the tendency towards longer wet and dry periods, would also affect discharge and loading estimates. Both higher temperatures and longer storm durations would contribute to wetter conditions in the watershed, producing antecedent conditions where soils are more saturated and the watershed is more vulnerable to any precipitation event, even if not extreme in nature. Contrasting model results from the WG versus GCM-driven model runs show that failure to capture changes in extreme precipitation in future climate scenarios translates to underestimation of the influence of increasing snowpack, higher peak discharges, and greater sediment yields. This result suggests using extreme caution when using GCM data for hydrological climate change impacts evaluation in the northeastern United States.

Variability in micrometeorological variables not included in our downscaled GCM inputs (windspeed, humidity, incoming

shortwave and longwave radiation) can be expected to influence a set of ecosystem processes (such as carbon and energy cycling, root uptake by plants, soil moisture, and others) that will impact water and sediment fluxes from watersheds. More comprehensive climate change simulations of these complex ecosystem interactions will require new methods to downscale these micrometeorological variables to subdaily timesteps. High resolution, distributed watershed modeling can help tease apart the specific processes that might be altered as a result of climate change. In this work we focused specifically on the effects of temperature and precipitation, while the effects of these other meteorological variables were not explored. Similarly, processes other than erosion may also be contributing to simulated sediment output, such as soil thawing and the effects of vegetation. These processes are not considered here.

No trends were seen in the ratio of modeled contributions of sediment from streambanks, roads, and overland erosion over time, either using WG or GCM driving data. While the lack of trends suggests that streambank collapse and incision do not begin to dominate sediment mobilization under more extreme precipitation (contrary to what is expected), it may also be that meteorological inputs were insufficient to characterize local climate changes at the resolution needed to see watershed response using this model. Alternatively, it may suggest that other factors could be driving the relative importance of bank failures in the watershed. Although high precipitation and flow events contribute to streambank erosion and failure, there is not a direct proportionality between the magnitude and frequency of the event and the rate or amount of erosion and failure. Wynn and Mostaghimi (2006) used regression analysis to evaluate which factors (including soil properties, antecedent conditions, root density, and freeze/thaw cycling) were most influential in determining erodibility and shear stress of streambanks. These authors found that soil bulk density had a crucial role in determining erodibility, among a number of other factors. It is likely that soil and stream characteristics held constant or determined using the same probability distributions in the runs presented in this work, have an important effect on soil erosion and failure processes in this watershed. Improved parameterization, including potentially tighter distributions of soil parameters such as bulk density, could alter how erosion mechanisms respond to meteorological inputs. It should also be noted that the ratio of sediment sources examined for this work were annual average ratios of sediment transported to the outlet of the watershed. The relatively unchanging ratios could also be a result of the particle size bins and the preferential transport of finer sediment sizes. Looking at the ratio of sediment from these sources on an event or seasonal basis would likely show more variability. Similarly, analysis at the subwatershed scale could also indicate different dynamics in the mechanisms that mobilize sediment.

5. Conclusions

Model results demonstrated that trends in regional precipitation and temperature both impact hydrological and sediment transport processes, where increasing temperatures resulted in earlier and higher spring melt and associated changes in discharge and sediment yield and simulated changes in precipitation resulted in higher and more frequent extreme discharge events and sediment yields. No significant changes in the ratios of sediment from streambank, road, and overland sources was observed, either because the model was not capturing the dynamics of sediment partitioning (possibly due to limitations in the driving data) or because other factors are driving the relative magnitude of bank erosion and failure in generating suspended sediment in this watershed.

Although simulating temperature and precipitation trends separately in this work allowed for comparison of the distinct impacts of changes in these driving factors, it limited assessment of the combined effects of trends in climate change in this region. The lack of available data that represent trends or changes in other meteorological variables, such as incoming solar radiation and wind, is also limiting. Changes in these other meteorological variables will likely occur with changing temperature and precipitation and will also impact hydrological and sediment responses in many watersheds. It was beyond the scope of this work to investigate relative contributions of sediment from streambank, road, and overland erosion at various time scales, but such an analysis might have provided more information on how these mechanisms might be altered as a result of changing flow regimes.

This work adds to the body of research that shows the influences of climate change on watershed processes that determine discharge and sediment loading, both of which are critical watershed management issues. Local increases in temperature can be expected to alter snow melt processes and flow regimes. Local increases in precipitation and extreme events can be expected to generate larger yields of suspended sediment. There is significant value in high resolution modeling of these processes to help understand potential changes that critically affect water quality of streams and rivers as well as receiving water bodies. However, such modeling requires high resolution meteorological data that represent expected changes in local climate, particularly in both temperature and precipitation. This work uses a new approach to simulating distributed bank erosion and failure within a watershed model to explicitly investigate the impacts of climate change on sediment fluxes. We conclude that local increases in temperature and precipitation are likely to increase sediment loading in the modeled watershed, as a result of changes in snow melt, an overall increase in wetter conditions, as well as in response to more extreme precipitation and flow events. The interaction of these influences is likely to create the most significant instances of bank erosion and sediment loading that would impact ecological systems, infrastructure, water quality, and other aspects of watershed health and sustainability. The ability to represent these mechanistic processes in a spatially explicit model environment offers new opportunities for identification of critical source and high risk areas, as well as an opportunity for further work to simulate the effects of targeted management or mitigation practices.

Funding

This research was supported by the Vermont Experimental Program for Stimulating Competitive Research (EPSCoR) and funded by NSF Awards EPS #1101317, Research on Adaptation to Climate Change in the Lake Champlain Basin (RACC) and OIA # 1556770, Basin Resilience to Extreme Events (BREE).

Conflicts of interest

None.

Appendix A. Supplementary data

Supplementary data associated with this article can be found, in the online version, at https://doi.org/10.1016/j.ejrh.2018.04.003.

References

Asselman, N.E.M., 1999. Suspended sediment dynamics in a large drainage basin: the River Rhine. Hydrol. Process. 13 (10), 1437–1450. http://dx.doi.org/10.1002/(SICI)1099-1085(199907)13:10<1437:AID-HYP821>3.0.CO;2-J.

Bagnold, R.A., 1966. An approach of sediment transport model from general physics. US Geol. Survey Prof. Paper 422-J.

Barg, L., Blazewicz, M., 2003. Asssessment of Fluvial Geomorphology in Relation to Erosion and Landslides in the Mad River Watershed in Central Vermont. Prepared for Vermont Geological Survey.

Betts, A., 2011. Climate change in Vermont. Climate Change Adaptation White Paper Series. Climate Change Team, Vermont Agency of Natural Resources.

Bowling, L.C., Storck, P., Lettenmaier, D.P., 2000. Hydrologic effects of logging in western Washington, United States. Water Resour. Res. 36 (11), 3223–3240. http://dx.doi.org/10.1029/2000WR900138.

Brekke, L., Thrasher, B., Maurer, E.P., Pruitt, T., 2013. Downscaled CMIP3 and CMIP5 climate projections: release of downscaled CMIP5 climate projections, comparison with preceding information, and summary of user needs. USBR Tech. Memo.

Chow, D.H.C., Levermore, G., 2007. New algorithm for generating hourly temperature values using daily maximum, minimum and average values from climate models. Build. Serv. Eng. Res. Technol. 28 (3), 237–248. http://dx.doi.org/10.1177/0143624407078642.

Cuo, L., Lettenmaier, D.P., Alberti, M., Richey, J.E., 2009. Effects of a century of land cover and climate change on the hydrology of the Puget Sound basin. Hydrol. Process. 23 (6), 907–933. http://dx.doi.org/10.1002/hyp.7228.

DeWolfe, M., Hession, W., Watzin, M., 2004. Sediment and phosphorus loads from streambank erosion in Vermont, USA. Crit. Trans. Water Environ. Resour. Manag., vol. 436. pp. 1–10.

Doten, C.O., Bowling, L.C., Lanini, J.S., Maurer, E.P., Lettenmaier, D.P., 2006. A spatially distributed model for the dynamic prediction of sediment erosion and transport in mountainous forested watersheds. Water Resour. Res. 42 (4). http://dx.doi.org/10.1029/2004WR003829.

Dunn, R.K., Springston, G.E., Donahue, N., 2007a. Surficial Geologic Map of the Mad River Watershed, Vermont (Northern Sheet).

Dunn, R.K., Springston, G.E., Donahue, N., 2007b. Surficial Geology Map of the Mad River Watershed, Vermont (Southern Sheet).

El-Khoury, A., Seidou, O., Lapen, D.R., Que, Z., Mohammadian, M., Sunohara, M., Bahram, D., 2015. Combined impacts of future climate and land use changes on discharge, nitrogen and phosphorus loads for a Canadian river basin. J. Environ. Manag. 151, 76–86. http://dx.doi.org/10.1016/j.jenvman.2014.12.012.

Fowler, H.J., Blenkinsop, S., Tebaldi, C., 2007. Linking climate change modelling to impacts studies: recent advances in downscaling techniques for hydrological modelling. Int. J. Climatol. 27 (12), 1547–1578. http://dx.doi.org/10.1002/joc.1556.

Frumhoff, P.C., Melillo, J.M., Moser, S.C., Wuebbles, D.J., 2007. Confronting climate change in the U.S. Northeast: science, impacts, and solutions. Synthesis Report of the Northeast Climate Impacts Assessment (NECIA). Union of Concerned Scientists (UCS), Cambridge, MA.

Gonzalez-Hidalgo, J.C., Batalla, R.J., Cerdà, A., de Luis, M., 2010. Contribution of the largest events to suspended sediment transport across the USA. Land Degrad. Dev. 21 (2), 83–91. http://dx.doi.org/10.1002/ldr.897.

Groisman, P.Y., Knight, R.W., Karl, T.R., 2001. Heavy precipitation and high streamflow in the contiguous United States: trends in the 20th century. Bull. Am. Meteorol. Soc. 82, 219–246.

Groisman, P.Y., Knight, R.W., Easterling, D.R., Karl, T.R., Hegerl, G.C., Razuvaev, V.N., 2005. Trends in intense precipitation in the climate record. J. Clim. 18 (9), 1326–1350. http://dx.doi.org/10.1175/JCLI3339.1.

Groisman, P.Y., Knight, R.W., Karl, T.R., 2012. Changes in intense precipitation over the central United States. J. Hydrometeorol. 13, 47–66.

Guilbert, J., Beckage, B., Winter, J.M., Horton, R.M., Perkins, T., Bomblies, A., 2014. Impacts of projected climate change over the Lake Champlain Basin in Vermont. J. Appl. Meteorol. Climatol. 53 (8), 1861–1875. http://dx.doi.org/10.1175/JAMC-D-13-0338.1.

Guilbert, J., Betts, A.K., Rizzo, D.M., Beckage, B., Bomblies, A., 2015. Characterization of increased persistence and intensity of precipitation in the northeastern United States. Geophys. Res. Lett. 42 (6). http://dx.doi.org/10.1002/2015GL063124. 2015GL063124.

Hamshaw, S., 2014. Suspended Sediment Prediction Using Artificial Neural Networks and Local Hydrometeorological Data, M.S., Thesis. University of Vermont, Burlington, VT.

Hayhoe, K., et al., 2006. Past and future changes in climate and hydrological indicators in the US Northeast. Clim. Dyn. 28 (4), 381–407. http://dx.doi.org/10.1007/s00382-006-0187-8.

Hayhoe, K., Wake, C., Anderson, B., Liang, X.-Z., Maurer, E., Zhu, J., Bradbury, J., DeGaetano, A., Stoner, A.M., Wuebbles, D., 2008. Regional climate change projections for the Northeast USA. Mitig. Adapt. Strateg. Glob. Change 13 (5–6), 425–436.

Hodgkins, G.A., James II, I.C., Huntington, T.G., 2002. Historical changes in lake ice-out dates as indicators of climate change in New England, 1850-2000. Int. J. Climatol. 22, 1819–1827. http://dx.doi.org/10.1002/joc.857.

Karl, T.R., Knight, R.W., 1998. Secular trends of precipitation amount, frequency, and intensity in the United States. Bull. Am. Meteorol. Soc. 79 (2), 231–241. http://dx.doi.org/10.1175/1520-0477(1998)079<0231:STOPAF>2.0.CO;2.

Karl, T.R., Melillo, J.T., Peterson, T.C., 2009. In: Karl, T.R., Melillo, J.T., Peterson, T.C. (Eds.), Global Climate Change Impacts in the United States. Cambridge University Press. https://downloads.globalchange.gov/usimpacts/pdfs/climate-impacts-report.pdf.

Katz, R.W., Brown, B.G., 1992. Extreme events in a changing climate: variability is more important than averages. Clim. Change 21 (3), 289–302. http://dx.doi.org/10.1007/BF00139728.

Kronvang, B., Grant, R., Laubel, A.L., 1997. Sediment and phosphorus export from a lowloand catchment: quantification of sources. Water Air Soil Pollut. 99 (1–4), 465–476. http://dx.doi.org/10.1023/A:1018347607 60.

Kronvang, B., Audet, J., Baattrup-Pedersen, A., Jensen, H.S., Larsen, S.E., 2012. Phosphorus load to surface water from bank erosion in a Danish lowland river basin. J. Environ. Qual. 41, 304–313. http://dx.doi.org/10.2134/jeq2010.0434.

Kunkel, K.E., Andsager, K., Easterling, D.R., 1999. Long-term trends in extreme precipitation events over the conterminous United States and Canada. J. Clim. 12 (8), 2515–2527. http://dx.doi.org/10.1175/1520-0442(1999)012<2515:LTTIEP>2.0.CO;2.

Kunkel, K.E., Stevens, L.E., Stevens, L., Sun, E., Janssen, D., Wuebbles, J., DeGaetano, A., Dobson, J.G., 2013. Regional climate trends and scenarios for the U.S. National Climate Assessment: part 1. climate of the northeast U.S. NOAA Technical Report NESDIS. National Oceanic and Atmospheric Administration, National Environmental Satellite, Data, and Information Service, Washington D.C.

Kunkel, K.E., 2003. North American trends in extreme precipitation. Nat. Hazards 29 (2), 291–305. http://dx.doi.org/10.1023/A:1023694115864.

Lake Champlain Basin Program, 2013. Flood Resilience in the Lake Champlain Basin and Upper Richelieu River.

Langendoen, E.J., Simon, A., Klimetz, L., Bankhead, N., Ursic, M.E., 2012. Quantifying sediment loadings from streambank erosion in selected agricultural watersheds draining to lake Champlain. NSL Technical Report No. 79. U.S. Dep. Of Agric. Natl. Sedimentation lab, Oxford, Mississippi.

Lanini, J.S., Clark, E.A., Lettenmaier, D.P., 2009. Effects of fire-precipitation timing and regime on post-fire sediment delivery in Pacific Northwest forests. Geophys.

Res. Lett. 36 (1), L01402. http://dx.doi.org/10.1029/2008GL034588.
Leung, L.R., Wigmosta, M.S., 1999. Potential climate change impacts on mountain watersheds in the Pacific Northwest. JAWRA J. Am. Water Resour. Assoc. 35 (6), 1463–1471. http://dx.doi.org/10.1111/j.1752-1688.1999.tb04230.x.
Maurer, E.P., Woods, A.W., Adams, J.C., Lettenmeier, D.P., Nijssen, B., 2002. A long-term hydrologically based dataset of land surface fluxes and states for the conterminous United States. J. Clim. 15 (20), 3237–3251. http://dx.doi.org/10.1175/1520-0442(2002)015<3237:ALTHBD>2.0.CO;2.
Mittelstet, A.R., Storm, D.E., Fox, G.A., 2016. Testing of the modified streambank erosion and instream phosphorus routines for the SWAT model. JAWRA 53 (1), 101–114.
Mohammed, I.N., Bomblies, A., Wemple, B.C., 2015. The use of CMIP5 data to simulate climate change impacts on flow regime within the Lake Champlain Basin. J. Hydrol. Reg. Stud. 3, 160–186. http://dx.doi.org/10.1016/j.ejrh.2015.01.002.
Morrissey, L.A., Rizzo, D.M., Ross, D.S., Alves, C., 2011. Quantifying Sediment Loading Due To Stream Bank Erosion in Impaired and Attainment Watersheds in Chittenden County, VT Using Advanced GIS and Remote Sensing Technologies. Project ID 2009VT44B U.S. Geol. Surv.
Moss, R.H., et al., 2010. The next generation of scenarios for climate change research and assessment. Nature 463 (7282), 747–756. http://dx.doi.org/10.1038/nature08823.
Moss, B., 2012. Cogs in the endless machine: lakes, climate change and nutrient cycles: a review. Sci. Total Environ. 434, 130–142. http://dx.doi.org/10.1016/j.scitotenv.2011.07.069.
Nagle, G.N., Fahey, T.J., Ritchie, J.C., Woodbury, P.B., 2007. Variations in sediment sources and yields in the Finger Lakes and Catskills regions of New York. Hydrol. Process. 21 (6), 828–838. http://dx.doi.org/10.1002/hyp.6611.
Oeurng, C., Sauvage, S., Sánchez-Pérez, J.-M., 2010. Dynamics of suspended sediment transport and yield in a large agricultural catchment, southwest France. Earth Surf. Process. Landf. 35 (11), 1289–1301. http://dx.doi.org/10.1002/esp.1971.
Pealer, S., 2012. Lessons from Irene: Building Resiliency as we Rebuild.
Prudhomme, C., Reynard, N., Crooks, S., 2002. Downscaling of global climate models for flood frequency analysis: where are we now? Hydrol. Proc. 16 (6), 1137–1150.
Safeeq, M., Fares, A., 2012. Hydrologic response of a Hawaiian watershed to future climate change scenarios. Hydrol. Process. 26 (18), 2745–2764. http://dx.doi.org/10.1002/hyp.8328.
Scharmer, K., Greif, J., 2000. The European Solar Radiation Atlas, Vol. 1: Fundamentals and Maps. Les Presses de l'Ecole des Mines, Paris.
Simon, A., Curini, A., Darby, S.E., Langendoen, E.J., 2000. Bank and near-bank processes in an incised channel. Geomorphology 35 (3–4), 193–217.
Simon, A., Langendoen, E.J., Thomas, R., 2003. Incorporating Bank-Toe Erosion by Hydraulic Shear into a Bank-Stability Model: Missouri River, Eastern Montana.
Simon, A., Pollen-Bankhead, N., Thomas, R.E., 2011. Development and application of a deterministic Bank Stability and Toe Erosion Model for stream restoration. In: Simon, A., Bennett, S.J., Castro, J.M. (Eds.), Stream Restoration in Dynamic Fluvial Systems. American Geophysical Union, pp. 453–474.
Stager, J.C., Thill, M., 2010. Climate Change in the Champlain Basin: What Natural Resource Managers can Expect and Do. The Nature Conservancy.
Stryker, J., Bomblies, A., Wemple, B., 2017. Modeling sediment mobilization using a distributed hydrology model coupled with a bank stability model. Water Resour. Res. 53 (6), 2051–2073. http://dx.doi.org/10.1002/2016WR019143.
US EPA, O, 2012. Channel Processes: Streambank Erosion. Available from: http://water.epa.gov/scitech/datait/tools/warsss/streamero.cfm. (Accessed 6 July 2015).
Walter, R.C., Merritts, D.J., 2008. Natural streams and the legacy of water-powered mills. Science 319 (5861), 299–304. http://dx.doi.org/10.1126/science.1151716.
Watzin, M.C., Fuller, S., Bronson, L., Gorney, R., Schuster, L., 2010. Monitoring and evaluation of cyanobacteria in Lake Champlain. Lake Champlain Basin Program, Technical Report. Lake Champlain Basin Program and Vermont Agency of Natural Resources, Grand Isle, VT.
Webb, B.W., Walling, D.E., 1982. The magnitude and frequency characteristics of fluvial transport in a devon drainage basin and some geomorphological implications. Catena 9 (1), 9–23. http://dx.doi.org/10.1016/S0341-8162(82)80002-7.
Wehner, M.F., Smith, R.L., Bala, G., Duffy, P., 2010. The effect of horizontal resolution on simulation of very extreme US precipitation events in a global atmosphere model. Clim. Dyn. 34 (2–3), 241–247. http://dx.doi.org/10.1007/s00382-009-0656-y.
Whalen, T.N., 1998. Post-Glacial Fluvial Terraces in the Winooski Drainage Basin, Vermont, M.S Thesis. University of Vermont, Burlington, VT.
Whitaker, A., Alila, Y., Beckers, J., Toews, D., 2002. Evaluating peak flow sensitivity to clear-cutting in different elevation bands of a snowmelt-dominated mountainous catchment. Water Resour. Res. 38 (9), 1172. http://dx.doi.org/10.1029/2001WR000514.
Whitehead, P.G., Wilby, R.L., Battarbee, R.W., Kernan, M., Wade, J., 2009. A review of the potential impacts of climate change on surface water quality. Hydrol. Sci. J. 54 (1), 101–123. http://dx.doi.org/10.1623/hysj.54.1.101.
Wicks, J.M., Bathurst, J.C., 1996. SHESED: a physically based, distributed erosion and sediment yield component for the SHE hydrological modeling system. J. Hydrol. 175, 213–238.
Wigmosta, M.S., Vail, L.W., Lettenmaier, D.P., 1994. A distributed hydrology-vegetation model for complex terrain. Water Resour. Res. 30 (6), 1665–1679. http://dx.doi.org/10.1029/94WR00436.
Williams, G.P., 1989. Sediment concentration versus water discharge during single hydrologic events in rivers. J. Hydrol. 111 (1), 89–106. http://dx.doi.org/10.1016/0022-1694(89)90254-0.
Winter, J.M., Beckage, B., Bucini, G., Horton, R.M., Clemins, P.J., 2016. Development and evaluation of high-resolution climate simulations over the mountainous Northeastern United States. J. Hydrometeorol. 17 (3), 881–896. http://dx.doi.org/10.1175/JHM-D-15-0052.1.
Wynn, T., Mostaghimi, S., 2006. The effects of vegetation and soil type on streambank erosion, southwestern Virginia, USA. JAWRA 42 (1), 69–82.
Xu, C., 1999. From GCMs to river flow: a review of downscaling methods and hydrologic modelling approaches. Prog. Phys. Geogr. 23 (2), 229–249. http://dx.doi.org/10.1177/030913339902300204.
Xu, C., Wilden, E., Halldin, S., 2005. Modelling hydrological consequences of climate change—progress and challenges. Adv. Atmos. Sci. 22 (6), 789–797.